Theoretical Investigation of the Imprinting Efficiency of Molecularly Imprinted Polymers

Simcha Srebnik

Department of Chemical Engineering, Technion−Israel Institute of Technology, Haifa 32000, Israel

Received July 30, 2003. Revised Manuscript Received December 29, 2003

Molecular imprinting is an emerging tool for the design of structured porous materials having a precise arrangement of functional groups within pores of a controlled size and shape. Such controlled specificity in principle can offer a scope of opportunities for molecule-specific recognition applications. In practice, however, molecular recognition is often not fully realized, either due to distortion during the imprinting process or due to incomplete imprinting. Using a mean-field lattice model, we study imprinting efficiency of tetrafunctional monomers using stiff imprinting agents of various sizes and for various preparation conditions. Neglecting imperfections and distortions during gelation and post-treatment, we show that high imprinting efficiencies (i.e., a large number of pores of the needed size and functionality) are hard to achieve. However, monomer−template interactions and preparation conditions can be optimized for a given template size to yield a higher population of high affinity sites.

Introduction

In the past 2 decades methods for tailoring the structure and chemical affinity of gels have advanced significantly, with particular attention focused on substance-specific recognition-based applications. Molecular imprinting is a technique that was developed to mimic recognition processes in biological systems. The method involves complexation of organic or inorganic functional monomers and organic templates (or print molecules), followed by cross-linking of the monomers and subsequent removal of the templates, thus incorporating molecule-specific binding sites in the gel. Recognition then occurs via a combination of reversible binding (covalent or polar) and shape complementarity with high affinity and selectivity. In fact, in many cases the technique has proven to be capable of producing materials with rebinding affinities and selectivities of the same order of magnitude as commonly observed for antibody−antigen interactions.[1] Applications include analysis and separation of trace levels of compounds, sensors, and enzyme mimics (e.g., refs 2 and 3). In addition, the molecular imprinting technique has been used to form ordered and structured (usually inorganic) gels (e.g., refs 4−9) Some distinct advantages of molecular imprinting include the simple and rapid preparation, the stability of the imprinted structures, and the wide variety of substances amenable to imprinting.

A notable difficulty with recognition-based applications of molecular imprinting is the low yields of high-affinity sites. The quality and performance of the imprinted gel is clearly affected by the physical and chemical nature of the monomers and templates and the interactions between them, by the polymerization reaction, and by the rebinding ability. Therefore, an understanding of the physics governing the formation of monomer−template complexes is fundamental to a strategic design of imprinted polymers. Nevertheless, although a rapidly growing field, few efforts have focused on characterizing and understanding the mechanisms underlying formation and recognition, and even fewer theoretical efforts have emerged that investigate the interplay of the various parameters influencing the molecular imprinting process.

Andersson et al.[10,11] studied the effect of monomer−template molar ratio on the selectivity of the imprinted gel. They found that low ratios result in less than optimal complexation due to insufficient amounts of functional monomers, and selectivity is thus reduced. On the other hand, excess monomer yields a high number of noncomplexed, randomly distributed monomers, which contribute to nonspecific binding. They introduced a semiempirical correlation for the estimation of the number of selective recognition sites in an imprinted polymer prepared with a given monomer−template ratio. Mosbach led systematic studies on the

(1) Sellergren, B. *TrAC, Trends Anal. Chem.* **1997**, *16*, 310.
(2) Collinson, M. M. *Crit. Rev. Anal. Chem.* **1999**, *29*, 289.
(3) Nicholls, I. A.; Adbo, K.; Andersson, H. S.; Andersson, P. O.; Ankarloo, J.; Hedin-Dahlstrom, J.; Jokela, P.; Karlsson, J. G.; Olofsson, L.; Rosengren, J.; Shoravi, S.; Svenson, J.; Wikman, S. *Anal. Chim. Acta* **2001**, *435*, 9.
(4) Hedrick, J. L.; Miller, R. D.; Hawker, C. J.; Carter, K. R.; Volksen, W.; Yoon, D. Y.; Trollsas, M. *Adv. Mater.* **1998**, *10*, 1049.
(5) Kramer, E.; Forster, S.; Goltner, C.; Antonietti, M. *Langmuir* **1998**, *14*, 2027.
(6) Boury, B.; Corriu, R. J. P.; Le Strat, V. *Chem. Mater.* **1999**, *11*, 2796.
(7) Lu, Y. F.; Cao, G. Z.; Kale, R. P.; Prabakar, S.; Lopez, G. P.; Brinker, C. J. *Chem. Mater.* **1999**, *11*, 1223.
(8) Nakanishi, K. *J. Sol-Gel Sci. Technol.* **2000**, *19*, 65.
(9) Hentze, H. P.; Antonietti, M. *Curr. Opin. Solid State Mater. Sci.* **2001**, *5*, 343.
(10) Andersson, H. S.; Nicholls, I. A. *Bioorg. Chem.* **1997**, *25*, 203.
(11) Andersson, H. S.; Karlsson, J. G.; Piletsky, S. A.; Koch-Schmidt, A. C.; Mosbach, K.; Nicholls, I. A. *J. Chromatogr. A* **1999**, *848*, 39.

10.1021/cm034705m CCC: $27.50
Published on Web 02/07/2004

effect of interactions on site affinity, which showed that high-affinity sites are increased with increasing interaction strength for noncovalent bonding.[12−14] The importance of multipoint interactions of different nature that stabilize the template−monomer complex was also realized.[15] Shea et al. studied the influence of template shape[16] and functional groups.[17]

Some theoretical studies have been published that focus on general aspects of molecular imprinting. For example, Nicholls et al.[3] used qualitative thermodynamic arguments to shed light on observed recognition behavior. Lu et al.[7] approximated the volume occupied by a propyl methacrylate molecule, the imprint agent. By comparison with experimental porosity measurements, they determined the percolation threshold volume fraction needed for accessibility of the pores created by removal of the agents. Enoki et al.[18] studied the effects of frustration on molecular imprinting involving copolymerization of functional ligands (that interact with the imprint molecule) and backbone monomers, followed by cross-linking. They conclude that post-cross-linking in the presence of the target molecule minimizes frustration and thus allows the imprinted copolymer gel to approach its free energy minimum and that the affinity toward the target molecule increases exponentially with increasing concentrations of post-cross-linking agents. They modeled this behavior using simple probabilistic arguments. Using mean-field theory, we[19−21] investigated the induced porosity of polymer networks obtained through various imprinting approaches, concentrating on the induced porous structure of the final imprinted gel under various preparation conditions.

In this work, we introduce a measure of imprinting efficiency (a measure of the degree of complexation) and study the effect of size and functionality of the imprinting agent on the imprinting efficiency using a lattice model. We concentrate on the effect of solvent−template−monomer interactions on the equilibrium population of monomer−template complexes. The extent of template complexation at equilibrium is governed by the change in Gibbs free energy of formation for each mode of template−monomer interactions, generally resulting in a population of sites with various affinities for the print molecule. Neglecting template−template association, we find that stronger template−monomer interactions results in higher functional complexes and thus higher imprinting efficiencies, in agreement with experiments. However, the efficiency strongly depends on the preparation conditions.

Theoretical Model

Corrales and Keefer[22] analyzed the complexation of metal oxides in a silica network using simple statistical mechanics calculations. We use a similar development to study the equilibrium template−monomer complexes of imprinting molecules within a network. The model developed below is general inasmuch as it applies to any tetrafunctional precursor and can easily be extended to monomers of various functionalities. An amorphous gel would consist of cross-linked monomers, Q^n, of various degrees of solvation, n, where the superscript denotes the number of cross-linking bonds. Of course, for an ideal network with no defects the network consists entirely of Q^4 monomers (ignoring surface groups). Now, consider a template molecule, T, having x functional ("cross-linking") sites. Then at chemical equilibrium, the following "bond-breaking" reactions can be said to take place that would lead to complexation of the print molecules and the formation of the following Q species

$$Q^n + jT^m \overset{K_n}{\longleftrightarrow} Q^{n-j}T_j^{m+1} + \text{leaving group} \xrightarrow{\text{heat}} Q^{n-j} \quad (1)$$

where the index $n \in \{0, ..., 4\}$, $j \in \{1, ..., n\}$, and $m \in \{0, ..., x - 1\}$. In writing eq 1, we assumed that only one site per print molecule can interact with a monomer. Further, we assume that the leaving group is small and no further bond-forming or breaking reactions take place after removal of the imprinting molecules. At equilibrium, the chemical equilibrium constants can be written in terms of the activities of the different species, such that for eq 1 we can write

$$K = \frac{a_{n-j}}{a_n a_T^j} \quad (2)$$

where a_i refers to the activity of the $Q^{i\text{th}}$ species and a_T is the activity of the monomer−template complex. The equilibrium constants are related to the thermodynamic Gibbs' free energy in the regular manner: $k_B t \ln K_n = \Delta G_n{}^0 = \Delta H_n{}^0 - t\Delta S_n{}^0$, where k_B is Boltzmann's constant and t is the temperature and ideal mixing (no volume change) is assumed.

The statistical model is built by placing the different species one by one on a tetrahedral lattice, where the volume of each site is equivalent to the volume occupied by a monomer. We define the size of the template, T, and thus the size of the cavities that remain in the network, in terms of the number of lattice sites that they occupy, r. Thus, r is the volume ratio of the print molecule to a monomer. The system is depicted in Figure 1.

In the following development, we consider a dilute concentration of the print molecules of functionality x and assume that no network defects exist. In other words, all templates are fully or partially associated. Letting n_T be the total number of templates, it follows that the total possible number of bonds between the monomers and the templates is xn_T. Denoting the number of templates that have i associated functional sites as n_{T_i} and assuming that, at equilibrium, $i \neq 0$ (no free print molecules), then the total number of

(12) Andersson, L. I.; Muller, R.; Vlatakis, G.; Mosbach, K. *Proc. Natl. Acad. Sci. U.S.A.* **1995**, *92*, 4788.
(13) Andersson, H. S.; KochSchmidt, A. C.; Ohlson, S.; Mosbach, K. *J. Mol. Recognit.* **1996**, *9*, 675.
(14) Berglund, J.; Nicholls, I. A.; Lindbladh, C.; Mosbach, K. *Bioorg. Med. Chem. Lett.* **1996**, *6*, 2237.
(15) Sellergren, B.; Lepisto, M.; Mosbach, K. *J. Am. Chem. Soc.* **1988**, *110*, 5853.
(16) Shea, K. J.; Sasaki, D. Y. *J. Am. Chem. Soc.* **1989**, *111*, 3442.
(17) Shea, K. J.; Dougherty, T. K. *J. Am. Chem. Soc.* **1986**, *108*, 1091.
(18) Enoki, T.; Tanaka, K.; Watanabe, T.; Oya, T.; Sakiyama, T.; Takeoka, Y.; Ito, K.; Wang, G. Q.; Annaka, M.; Hara, K.; Du, R.; Chuang, J.; Wasserman, K.; Grosberg, A. Y.; Masamune, S.; Tanaka, T. *Phys. Rev. Lett.* **2000**, *85*, 5000.
(19) Srebnik, S.; Lev, O.; Avnir, D. *Chem. Mater.* **2001**, *13*, 811.
(20) Srebnik, S.; Lev, O. *J. Chem. Phys.* **2002**, *116*, 10967.
(21) Srebnik, S. Submitted to *J. Phys. Chem.*
(22) Corrales, L. R.; Keefer, K. D. *J. Chem. Phys.* **1997**, *106*, 6460.

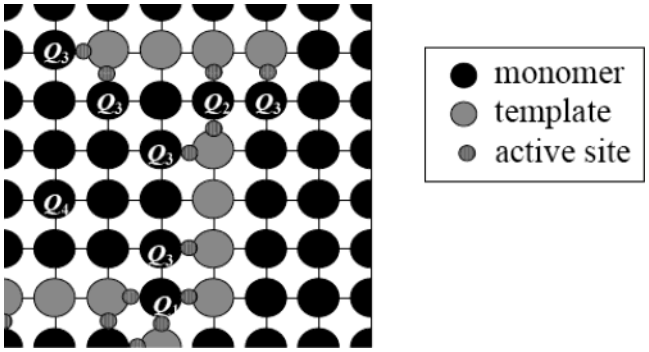

Figure 1. Schematic depiction of the modeled system. The monomers and print molecules are placed on a lattice. The *Q* species are represented by black circles while the removable functional print molecules are represented by gray circles. Only those *Q* species formed through bonding with functional sites on the templates are labeled for clarity. It is assumed that only Q^4 and Q^3 species exist, where the latter form as a result of monomer−template bonds.

templates is $n_T = \sum_{i=1}^{f} n_{T_i}$. Further, we assume that of the monomers, only Q^4 and Q^3 species exist (Q^4 corresponds to a fully cross-linked monomer while Q^3 corresponds to template-associated monomer and therefore there are no network defects), meaning that the concentration of the imprinting agents is relatively dilute, such that each monomer forms at most one bond with a print molecule. For a completely random process, this assumption is valid up to 10% volume fractions. The assumption breaks down quickly for $r = 1$; that is, for 40% volume fraction of templates only about 50% of the lattice is made up of Q^3 and Q^4 species. However, a simple simulation shows that as r increases (larger templates), the fraction of Q^3 and Q^4 species increases quickly to over 70% for $r = 5$ at 40% occupancy. In addition, conditions that tend to mix the templates and monomers (as are mostly considered in our study) will further increase the fraction of Q^3 and Q^4 species. Such a model allows for the prediction of the efficiency of the imprinting process as well as the volume fraction that can be occupied by the imprinting-induced cavities under thermodynamic equilibrium conditions. Following these assumptions, the partition function describing the number of possible states of the system can be written as

$$Z = \sum_{n} a_4^{n_4} a_{T_1}^{n_{T1}} a_{T_2}^{n_{T2}} \ldots a_{T_f}^{n_{Tf}} \Omega[n_4, n_T] \tag{3}$$

where Ω is the configurational entropy contribution, determined from the number of ways of placing a mixture of the different species on a lattice of N_s sites, given that they must be arranged in such a way that each print molecule forms at least one bond with a monomer and all monomers are otherwise fully cross-linked.

In the following derivation we consider the print molecules to be rigid rods made up of r units (each of size of the lattice monomer) and having four functional sites (the model can be easily modified for molecules of any number of functional sites). We calculate Ω for our system in the manner of Flory's lattice models[23,24] as follows. First, we note that Ω can be written as a conditional product of the number of ways of placing each of the imprinting agents that are solvated to different degrees, times the number of ways of placing the Q^4 species

$$\Omega = \Omega_1 \Omega_{2|1} \Omega_{3|2,1} \Omega_{4|3,2,1} \Omega_{Q^4|4,3,2,1} \tag{4}$$

where Ω_1 is the number of ways of placing templates associated with one monomer (T^1 species, each taking up $r + 1$ lattice sites), $\Omega_{2|1}$ is the number of ways of placing templates associated with two monomers (T^2), each taking up $r + 2$ lattice cells and given that T^1 species are on the lattice, and so forth. The last configurational contribution appearing in eq 4 is the number of ways of placing the Q^4 species on the lattice given that the various T species have been placed, which is simply unity since we are assuming a perfect gelation process. Further, $\Omega_k = (1/n_{T_k}!)\prod_{i=1}^{n_{Tk}} \nu_i^k$ where ν_i^k is the expected number of sets of $r + k$ contiguous sites available to the $i + 1$ species of type T^k and the factorial accounts for indistinguishability. The expression for ν_i^k can be derived in the usual manner,[23,24] and for our problem we obtain

$$\nu_{j+1}^k = (N_s - (r+1)j)z(1 - f_j)^r f \omega_k \tag{5}$$

where z is the coordination number of the lattice and ω_k is the number of distinguishable ways of placing templates having k associated functional sites. Thus, solving for Ω, we obtain

$$\Omega \approx \frac{N_s! 2^{2n_T} \omega_1^{n_{T1}} \omega_2^{n_{T2}} \omega_3^{n_{T3}} \omega_4^{n_{T4}}}{n_{T_1}! n_{T_2}! n_{T_3}! n_{T_4}! n_4! N_s^{N_s - n_4 - n_T}} \tag{6}$$

The Gibbs free energy is found by taking the logarithm of eq 3. Using Sterling's approximation, we obtain

$$\begin{aligned} \frac{G}{k_B t} \approx\ & n_4(\ln x_4 - \mu_4) + n_{M_1}\left(\ln\frac{x_{T_1}}{4\omega_1} - \mu_{T_1}\right) + \\ & n_{T_2}\left(\ln\frac{x_{T_2}}{4\omega_2} - \mu_{T_2}\right) + n_{T_3}\left(\ln\frac{x_{T_3}}{4\omega_3} - \mu_{T_3}\right) + \\ & n_{T_4}\left(\ln\frac{x_{T_4}}{4\omega_4} - \mu_{T_4}\right) + r n_{T_1} + (r+1) n_T + (r+2) n_{T_3} + \\ & (r+3) n_{T_4} + \chi_V n_3 + \chi_F r n_T (1 - r x_T) \end{aligned} \tag{7}$$

where $x_i = n_i/N_s$ and we have defined the activity of species k in terms of its chemical potential, μ_k, as $a_k = \exp(\mu_k/k_B t)$. The last two terms have been added to account for the energetic contribution of the template−monomer associating nonspecific and specific interactions, respectively.

At equilibrium the partial derivatives of the free energy with respect to the different species equals zero. From the isothermal differential of the free energy, given by $dG = \mu_4\, dn_4 + \mu_{T_1}\, dn_{T_1} + \mu_{T_2}\, dn_{T_2} + \mu_{T_3}\, dn_{T_3} + \mu_{T_4}\, dn_{T_4}$, we arrive at the following equations for the number fractions of the different species:

$$x_{T_1} = 4\omega_1 x_4^{r+1} e^{-\chi_V - r - \chi_F r(1 - 2r x_T)} \tag{8}$$

$$x_{T_2} = (\omega_2/\omega_1) x_4 e^{-\chi_V - 1} x_{T_1} \tag{9}$$

(23) Flory, P. J. *J. Chem. Phys.* **1942**, *10*, 51.
(24) Flory, P. J. *J. Chem. Phys.* **1944**, *12*, 425.

$$x_{T_3} = (\omega_3/\omega_1)x_4^2 e^{-2(\chi_V+1)}x_{T_1} \quad (10)$$

$$x_{T_4} = (\omega_4/\omega_1)x_4^3 e^{-3(\chi_V+1)}x_{T_1} \quad (11)$$

$$x_4 = 1 - (r+1)x_{T_1} - (r+2)x_{T_2} - (r+3)x_{T_3} - (r+4)x_{T_4} \quad (12)$$

$$x_T = x_{T_1} + x_{T_2} + x_{T_3} + x_{T_4} \quad (13)$$

Equations 8−13 are solved simultaneously for the equilibrium fraction of the various site populations and monomers for different values of r, χ_V, and χ_F.

Results and Discussion

The model allows us to obtain the equilibrium composition of the imprinted gel, assuming that there are no network defects apart for incomplete association of the functional sites of the print molecules. As has been observed experimentally, we find that the potential for a given monomer−template pair to produce templated sites depends on the stability of the complex or the nature of the binding sites[15,12] and that a wide population of cavities with different affinities exist.[25,12] The model treats different materials and preparation conditions through the interactions parameters χ_V, which is related to the excluded volume of the monomers, and χ_F, which is a measure of the difference in the interactions between the different materials (monomers and templates) and is proportional to the inverse of the temperature.[26] In our definition, χ_F vanishes when the interactions are similar in magnitude, it is negative when interactions between unlike species are unfavorable, and it is positive when the interactions are favorable. Thus, different values of the interaction parameters effectively correspond to different preparation conditions defined by the temperature and solvent.

The extent of "optimal" template coordination by a functional monomer is dependent upon the nature of each of the chemical components present in the system (i.e., monomer, template, and solvent) and upon the physical environment (e.g., temperature and pressure). The relative strengths of the monomer−template−solvent interactions influence the position of equilibrium and thus the extent and quality of functional monomer−template interactions, which in turn govern the quality of the resultant site population. Nevertheless, accomplished high-affinity binding sites are usually in the range of only a few percent, resulting in general in relatively nonspecific binding.[27] Our model provides insight into the origin of the low imprinting efficiencies for small template molecules whose recognition in such systems is thus based only on the defined interactions.

The formation of an imprinted porous material requires that the imprinting agents be removed after gelation. Consequently, since we assume highly crosslinked and rigid gels, the resulting cavities can be assumed to retain characteristics complementary to the templates. Thus, in our model, the limiting factor that determines the efficiency of the imprinting process is incomplete imprinting of the functional sites. In Figure 2a, we show the dependence of the fraction of imprinting agents that can be accommodated by the gel as a function of the size of the templates under various solution conditions. It is seen that the number of print molecules associated at equilibrium conditions decreases rapidly with increasing size. For most sizes, the theory suggests that good solvents for the print molecules ($\chi_V > 0$) tend to reduce the equilibrium fraction that can be incorporated into the gel, while strong template−monomer interactions ($\chi_F > 0$) tend to increase the fraction. Incidentally, the latter condition is also necessary to avoid aggregation of the imprinting agents. Interestingly, as is apparent from the first five curves (closed symbols and open squares), a proper combination of χ_V and χ_F could lead to somewhat higher volume fractions of incorporated imprinting agents at high molecular sizes! The results are seen more clearly by a plot of the volume fraction of imprinted cavities versus their size in Figure 2b. It is seen that the relative volume fraction of functional cavities can be increased substantially using a proper combination of χ_V and χ_F (e.g., open squares). These results are supported by Andersson et al.[10,11] who found less than optimal complexation when small amounts of functional monomers are used, leading to reduced selectivity. On the other

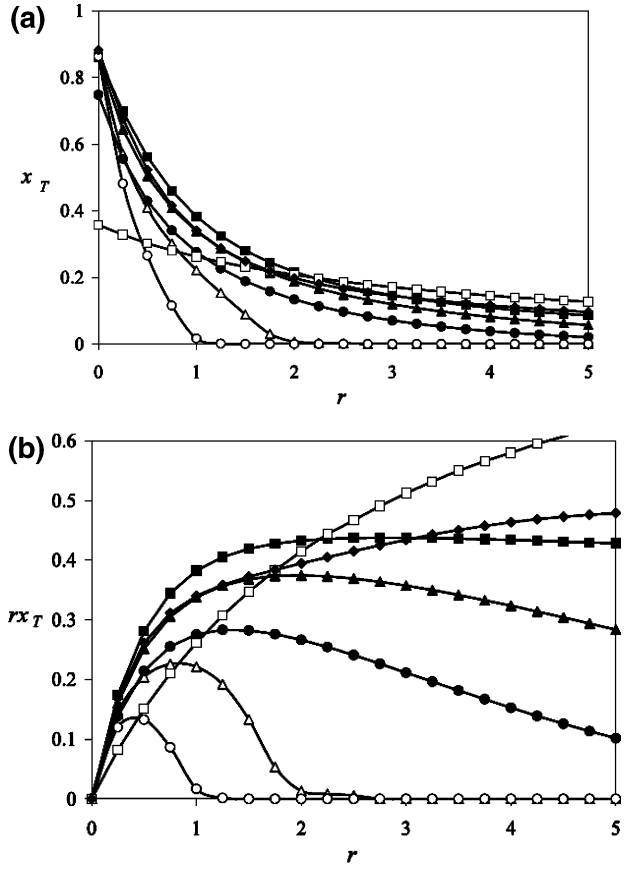

Figure 2. (a) Number fraction and (b) volume fraction of imprinted pores as a function of the size of the imprinting molecule. Curves correspond to (− ■ −) $\chi_V = \chi_F = 0$; (− ▲ −) $\chi_V = 2$, $\chi_F = 0$; (− ● −) $\chi_V = 2$, $\chi_F = 5$; (− ◆ −) $\chi_V = \chi_F = 5$; (− □ −) $\chi_V = 8$, $\chi_F = 5$; (− △ −) $\chi_V = 2$, $\chi_F = -5$; (− ○ −) $\chi_V = 2$, $\chi_F = -10$.

(25) Sellergren, B.; Ekberg, B.; Mosbach, K. *J. Chromatogr.* **1985**, *347*, 1.
(26) Orofin, T. A.; Flory, P. J. *J. Chem. Phys.* **1957**, *26*, 1067.
(27) Sellergren, B. *Angew. Chem., Int. Ed.* **2000**, *39*, 1031.

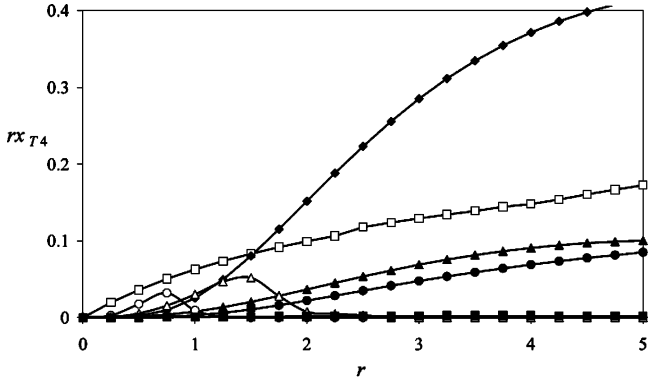

Figure 3. Volume fraction of fully functional pores as a function of pore size for various preparation conditions. Parameter values are identical to those given in Figure 2 (− ■ −) $\chi_V = \chi_F = 0$; (− ▲ −) $\chi_V = 2$, $\chi_F = 0$; (− ● −) $\chi_V = 2$, $\chi_F = 5$; (− ◆ −) $\chi_V = \chi_F = 5$; (− □ −) $\chi_V = 8$, $\chi_F = 5$; (− △ −) $\chi_V = 2$, $\chi_F = -5$; (− ○ −) $\chi_V = 2$, $\chi_F = -10$.

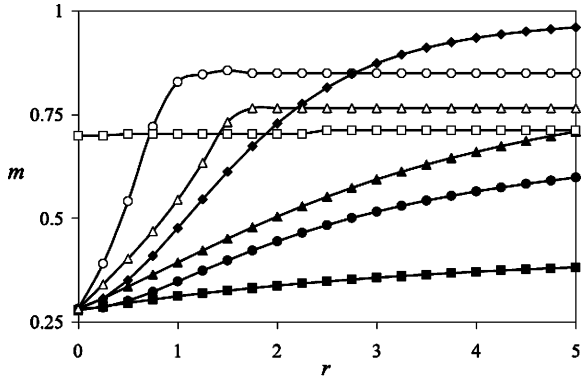

Figure 4. Order parameter indicating the fraction of imprinted pores that are fully functional. Parameter values are identical to those given in Figure 2 (− ■ −) $\chi_V = \chi_F = 0$; (− ▲ −) $\chi_V = 2$, $\chi_F = 0$; (− ● −) $\chi_V = 2$, $\chi_F = 5$; (− ◆ −) $\chi_V = \chi_F = 5$; (− □ −) $\chi_V = 8$, $\chi_F = 5$; (− △ −) $\chi_V = 2$, $\chi_F = -5$; (− ○ −) $\chi_V = 2$, $\chi_F = -10$.

hand, excess functional monomer−template ratios yield a high number of noncomplexed, randomly distributed monomers, resulting in nonspecific binding. That is, the degree of complexation between the templates and monomers (roughly measured by χ_F) greatly influences the imprinting efficiency.

The volume fractions of *fully functional* cavities of high affinity as a function of imprinting molecule size for the different preparation conditions are plotted in Figure 3. In contrast to the total number of imprinted cavities of Figure 2, it appears as if ideal solution conditions ($\chi_V = \chi_F = 0$, solid squares) hardly favor complete complexation of the templates and any deviation from such conditions increases the imprinting effect. Furthermore, it is seen that optimum conditions exist for a given size of the imprinting molecules (typified by a peak at a particular r). In addition, optimal solution conditions determined by the excluded volume of the monomers as well as type of the specific interactions (χ_F) appear to exist. Comparison of curves in Figure 3 show that, for $r > 2$, $\chi_V = 5$ (solid diamonds) proves to be more efficient than both $\chi_V = 2$ (solid circles) and $\chi_V = 8$ (open squares) for mixing conditions ($\chi_F = 5$). In addition, while mixing interactions may be favorable for larger templates, segregating interactions ($\chi_F < 0$) are favorable for small ones (open circles and triangles).

We can define the imprinting efficiency through use of an order parameter, m, which measures the number of associated functional sites, or degree of complexation of the imprinting agents, as

$$m = n_3/fn_M \begin{cases} < 1, \text{ partially functional imprint cavities} \\ = 1, \text{ fully functional imprint cavities} \end{cases} \quad (14)$$

The change of the order parameter with template size for the different preparation conditions in Figures 2 and 3 is plotted in Figure 4. It is seen that in general a plateau is reached in the imprinting efficiency for large r and that the plateau value differs for different conditions. Mixing conditions, which are favorable for imprinting since they discourage aggregation of the print molecules, result in very high imprinting efficiencies especially for high molecular weights. Yet by comparison with Figures 2 or 3, it is clear that very good solvents ($\chi_V > 5$) are needed for a sufficient fraction of imprinted pores; otherwise, low fractions of high-affinity cavities are formed.

The behavior of the different curves is clearly nonuniversal. For instance, it is seen that at one extreme a sharp transition from low to high values of the order parameter reminiscent of a phase transition is observed for conditions where interactions between the same species are favored over interactions between different species (open circles), while for strong mixing interactions there is no change in the order parameter for the range of sizes studied (open squares). In general, however, it is observed that the order parameter vanishes for small values of r since when the imprinting agents are small, x monomers must be in close vicinity and attach to the same small molecule and are thus sterically hindered. On the other hand, for agents greater than a critical size (of the order of the size of the lattice monomer) the length scale of the excluded volume repulsive interactions between the monomers attached to the same imprinting molecule during preparation is smaller than the distance between the monomers, and a further increase in molecular size does not alter this; thus, we observe a plateau. Stronger excluded volume interactions in effect increase the monomer size and delay the transition to larger values of r. An interesting case is when $\chi_F = 5$ and $\chi_V = 8$ (open squares). The strong interactions between the monomers and print molecules, on one hand, and the strong excluded volume interactions, on the other hand, lead to a nearly constant and high imprinting efficiency. That is, the more stable the template−monomer complex, the greater the number and fidelity of the resulting imprinted gel.

Plots of the relative concentrations of the different template complexes, x_{T_i}, in eqs 8−11, as a function of template size are shown in Figure 5. Comparing the inlay where there are no interactions between the template and monomers ($\chi_V = \chi_F = 0$) with the results in the main figure, where both the specific and nonspecific interactions are relatively strong ($\chi_V = \chi_F = 5$) clearly shows the important role of the nature of the interactions on the degree of complexation of the templates. Where in the former case fully associated

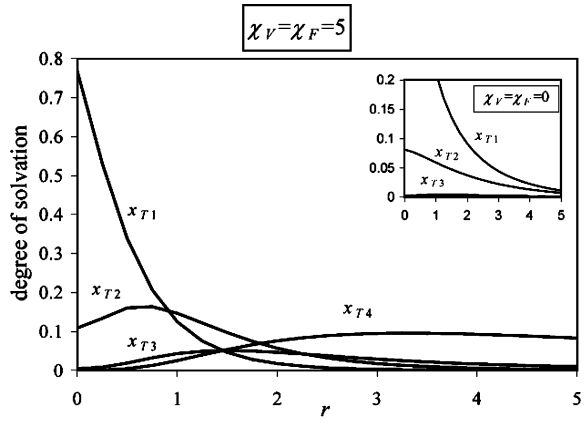

Figure 5. Relative population of cavities of different affinities as a function of template size, for $\chi_V = \chi_F = 5$ and for $\chi_V = \chi_F = 0$ (inlay).

templates are present in a very small amount, in the latter case we see that high-affinity monomer−template complexes actually dominate for template sizes corresponding to $r > 2$. This is significant since the extent of complexation directly influences polymer selectivity. In fact, experimental studies led by Mosbach regarding the effect of interactions on site affinity showed that the affinity increases with increasing interaction strengths[12−14] and that multipoint interactions of a different nature tended to stabilize the template−monomer complex.[15]

Conclusion

The binding site population in imprinted gels is often characterized by a small concentration of binding sites with high affinity and selectivity for the target analyte and a larger number of low affinity and less selective sites. Using a simple statistical thermodynamic model, it was shown that the fraction of imprinting-induced pores of the required functionality could be maximized for a particular size of the template using appropriate preparation conditions. In particular, high excluded volume conditions seem to favor small molecules, while strong monomer−template interactions favor templates of higher molecular sizes compared with the gel monomers. In addition, the theory suggests that optimal conditions exist for the equilibrium fraction of print molecules of a particular size that can be incorporated into the cross-linked gel. The findings of this study may be used as a qualitative guidance in the preparation of imprinting gels and can be easily tested through systematic experimental studies of molecular imprinting using agents of different sizes (r), chemical nature (χ_F), using different solvents (χ_V), for different preparation conditions (e.g., pH and temperature).

Acknowledgment. This research was supported, in part, by the Israel Science Foundation and the P. and E. Nathan Research Fund. The author acknowledges being a Koebner-Klein Scholar.

CM034705M